

# Deviation of Phase Difference and Frequency Dependent Energy Attenuation in Japan

Kenichi Nagao & Jun Kanda

University of Tokyo, Japan



## SUMMARY:

To determine the artificial ground motion, the information for the target response spectrum and phase angles are necessary. In current practice, phase angles are assumed to be random or phase angles of recorded seismic events are used. On the other hand, Ohsaki (1979) pointed out that the phase differences determine the nonstationarity of ground motion (the standard deviation of phase difference ( $\sigma$ ) is regarded as the duration of ground motion). In this study, the authors define the energy attenuation ( $E.A.$ ) as the ratio of energy at site to energy at the source and investigate the relationship between the  $\sigma$  and  $E.A.$  By defining the  $E.A.$ , one can take into account the heterogeneous  $Q$  and  $V_s$  structures. In the final part, the authors give some numerical examples to demonstrate the simulation method proposed in this study.

*Keywords: phase difference, energy attenuation, source spectrum*

## 1. INTRODUCTION

The peak amplitude, duration of strong motion and frequency content are the three most important characteristics of the earthquake ground motion. A huge number of researches on the strong motion duration have been done and many of them discuss about the relations between the duration and the earthquake magnitude, distance from the source, and so forth. On the other hand, in Japan, some studies investigated the statistical characteristics of the phase difference, especially the standard deviation (denoted as  $\sigma$  in this paper). The phase difference is defined as the difference between two neighboring phase angles. Ohsaki (1979) pointed out that the histogram of phase differences, which is called the phase difference distribution, has similar shape of the envelope of ground motion (see Fig.1). This is already explained mathematically (Papoulis (1977), Iwasaki *et al.* (1988), Yamane and Nagahashi (2002)). Hence,  $\sigma$  can be regarded as the duration of strong motion.

Further, the authors have investigated the characteristics of the skewness ( $\beta_3$ ) and kurtosis ( $\beta_4$ ) of phase difference. We have found that  $\sigma$  and  $\beta_3$ , and  $\sigma$  and  $\beta_4$  are well correlated (Nagao and Kanda (2012)). Therefore, if  $\sigma$  can be estimated accurately, values of  $\beta_3$  and  $\beta_4$  can be obtained.

In previous researches,  $\sigma$  is defined as linear functions of the hypocentral or epicentral distances. Generally, larger the distances are, longer the duration is and thus larger the  $\sigma$  is. While some earthquakes show clear relationships between the  $\sigma$  and distances, other earthquakes do not, as in Fig.2, for instance. Since the earthquake waves travel through the heterogeneous  $Q$  and  $V_s$  structures, it would not be appropriate to describe the  $\sigma$  simply as a function of distances. In this paper, the authors propose the Energy Attenuation,  $E.A.$ , as a tool to estimate  $\sigma$ . The  $E.A.$  represents the amount of energy decay

from the source to each site. The *E.A.* is computed from ground motion record, so it can consider such  $Q$  and  $V_s$  heterogeneities.

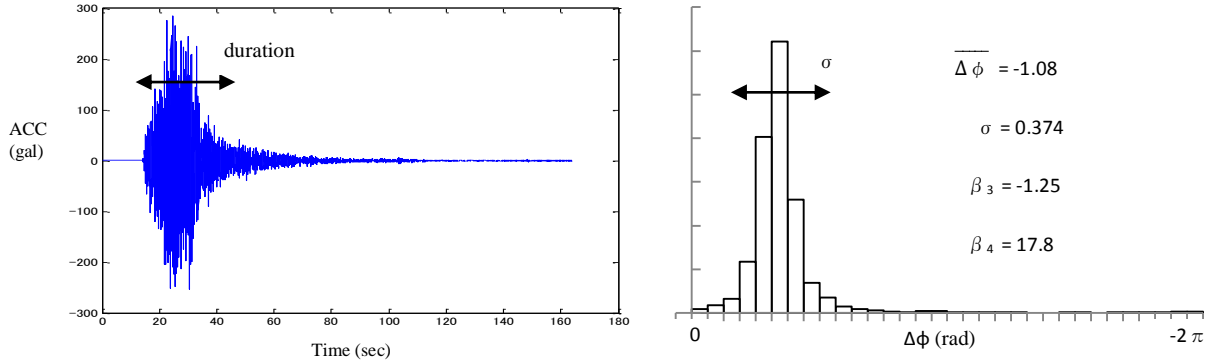


**Figure 1.** Examples of ground motion and its phase difference distribution

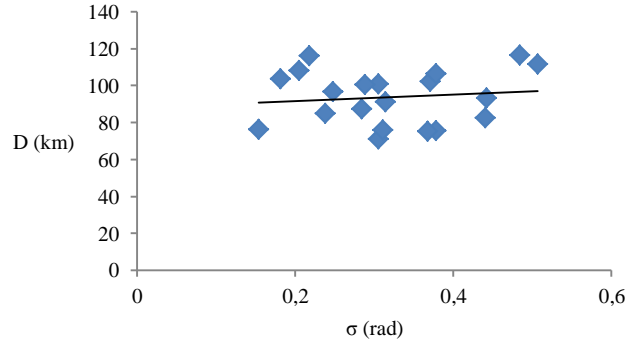


**Figure 2.** Example of  $\sigma - D$  relation ( $D$  is the hypocentral distance)

## 2. DEFINITIONS

The *E.A.* can be defined follows:

$$E.A. \text{ in a frequency band} = \frac{\sum F_{site}^2(f) \text{ in the frequency band}}{\sum F_{source}^2(f) \text{ in the frequency band}} \quad (2.1)$$

Where  $F_{site}(f)$  is the Fourier amplitude of the ground motion at a site and  $F_{source}(f)$  is the Fourier amplitude at a source. The  $f$  is the frequency. For  $F_{source}(f)$ , the source spectrum proposed by Boore (1983) is used:

$$F_{source}(f) = \frac{R_{\theta\phi} F_S P_{RTITIN}}{4\pi\rho\beta^3} M_0 \frac{\omega^2}{1+(\omega/\omega_c)^2} \left[1 + (\omega/\omega_m)^{2s}\right]^{-0.5} \quad (2.2)$$

Where  $R_{\theta\phi}$  is the radiation pattern,  $F_S$  is the amplification due to the free surface,  $P_{RTITIN}$  is the reduction factor,  $\rho$  is the density,  $\beta$  is the shear wave velocity,  $\omega_c$  is the corner frequency,  $\omega_m$  is the cutoff frequency and  $M_0$  is the seismic moment. For  $F_{site}(f)$ , if ground motion record is obtained on layer where  $V_s > 2000$  m/s,  $F_{site}(f)$  is set equal to  $F_{record}(f)$ , where  $F_{record}(f)$  is the Fourier amplitude of the ground motion record itself. Otherwise,  $F_{site}(f)$  is defined as  $F_{record}(f)/T(f)$ , where  $T(f)$  is the transfer function from

the shallowest point where  $V_s > 2000$  m/s to the location of the accelerogram. The  $T(f)$  is computed using the one-dimensional multiple reflection theory (The  $T(f)$  is only for shear wave).

The Fourier amplitude decay from the source can be represented as the following equation:

$$\sqrt{E.A.} = \frac{1}{D} \exp\left(\frac{-\pi*f*D}{\bar{Q}*\bar{V}_s}\right) = \frac{1}{D} \exp\left(\frac{-\pi*f}{\bar{Q}}\right)^{\frac{D}{\bar{V}_s}} \quad (2.3)$$

Where  $D$  is the hypocentral distance,  $\bar{Q}$  is the ‘‘average’’ quality factor and  $\bar{V}_s$  is the ‘‘average’’ shear wave velocity from the source to a site. Obviously, the ground motion travels through the heterogeneous  $Q$  and  $V_s$  structures and the  $E.A.$  can be affected by them as well as  $D$ . To consider the effect from the  $\bar{Q}$  value, the authors individually estimated the  $\bar{V}_s$  by looking at each of the records in this study and computed  $\frac{-\pi*f}{\bar{Q}}$ . The  $\bar{V}_s$  values are not significantly different among sites in the same earthquake event. Then each site was classified according to the  $\frac{-\pi*f}{\bar{Q}}$  values. This classification is used to estimate the  $E.A.$  from  $D$ .

$$\text{Group 1: if } \frac{-\pi*f}{\bar{Q}} \leq -0.09960$$

$$\text{Group 2: if } -0.09960 < \frac{-\pi*f}{\bar{Q}} \leq -0.07472$$

$$\text{Group 3: if } -0.07472 < \frac{-\pi*f}{\bar{Q}} \leq -0.04982$$

$$\text{Group 4: if } -0.04982 < \frac{-\pi*f}{\bar{Q}} \leq -0.02491$$

$$\text{Group 5: if } -0.02491 < \frac{-\pi*f}{\bar{Q}} \leq 0$$

$$\text{Group 6: if } 0 < \frac{-\pi*f}{\bar{Q}}$$

### 3. GROUND MOTIONS AND PARAMETERS USED IN THIS STUDY

The authors chose 13 earthquakes as in Table.1. For each earthquake, a huge number of records are obtained. In this study, the authors analyzed records obtained within 100 km epicentral distance. However, the three interface earthquakes occurred off the coast of the Pacific Ocean and the numbers of records within 100 km are very few. For that reason, the authors used records up to 150 km for 2005 Miyagiken oki earthquake and 200 km for 2003 Tokachi oki and 2011 Sanriku oki earthquake.

For parameters used in Eqn.2.2, the authors used  $\rho = 2.7$  g/cm<sup>3</sup> for crustal earthquakes and 3.0 g/cm<sup>3</sup> for the other two types,  $\beta = 3.4$  km/s for crustal earthquakes and 4.0 km/s for the other two,  $\omega_m = 6.0*2\pi$  rad/sec for crustal earthquakes and  $13.5*2\pi$  rad/sec for the other two types,  $R_{\theta\phi} = 0.63$ ,  $F_s = 2$ ,  $P_{RTITIN} = 1$  (all of them as in (Sato (2007))) and  $s = 4$  (Boore (1983)).  $M_0$  and  $\omega_c$  are determined from the moment magnitudes and stress drops estimated from other studies. For frequency bands considered in this study are 0.1 – 1.0 Hz, 1.0 – 2.0 Hz, 2.0 – 3.0 Hz, 3.0 – 5.0 Hz and 5.0 -10.0 Hz.

Some earthquakes (2004 Niigataken chuetsu, 2007 Notohanto oki, 2007 Niigataken chuetsuoki, 2008 Iwate-Miyagi nairiku, 2003 Tokachi oki, 2005 Miyagiken oki, 2011 Sanriku oki, 2001 Iwateken nairiku nanbu, 2003 Miyagiken oki and 2009 Surugawan earthquakes) include sites where layers with  $V_s > 2000$  m/s are located more than 450 m from the ground surface. In other words, those sites are located on thick

sedimentary layers. In sedimentary layers, the long-period surface waves can be less amplified (Nishikawa *et al.* (2008)). Although the site effect is already considered by defining  $T(f)$ , the  $T(f)$  cannot take the surface wave amplification, since the  $T(f)$  was only considered for the shear wave.

Based on this assumption, the authors developed the  $\sigma$  and  $E.A.$  relations in 0.1 – 1.0 Hz for the sedimentary and non-sedimentary sites.

**Table 1.** Earthquakes' data analyzed in this thesis

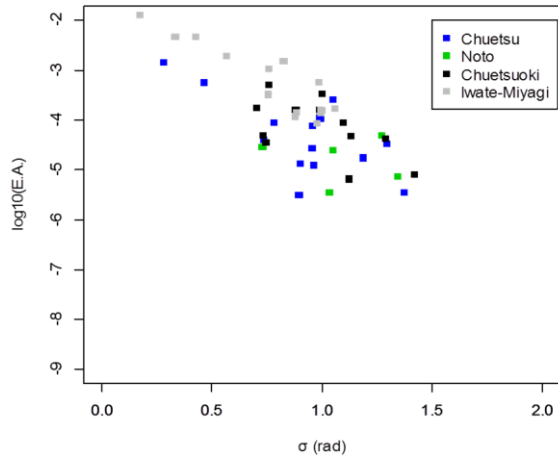
No.	Name	Occurrence date	$M_w$	Depth	Mechanism	Hypocenter location
1	Tottoriken seibu	2000/10/06	6.6	11 km	Crustal, strike	Long. 133.35 Lat. 35.28
2	Niigataken chuetsu	2004/10/23	6.6	13 km	Crustal, reverse	Long. 138.87 Lat. 37.29
3	Fukuokaken seihouoki	2005/03/20	6.6	9 km	Crustal, strike	Long. 130.18 Lat. 33.74
4	Notohanto oki	2007/03/25	6.7	11 km	Crustal, reverse	Long. 136.69 Lat. 37.22
5	Niigataken chuetsu oki	2007/07/16	6.6	17 km	Crustal, reverse	Long. 138.61 Lat. 37.56
6	Iwate - Miyagi nairiku	2008/06/14	6.9	8 km	Crustal, reverse	Long. 140.88 Lat. 39.03
7	Tokachi oki	2003/09/26	7.9	42 km	Interface, reverse	Long. 144.07 Lat. 41.78
8	Miyagiken oki	2005/08/16	7.1	45 km	Interface, reverse	Long. 142.28 Lat. 38.15
9	Sanriku oki	2011/03/09	7.2	8 km	Interface, reverse	Long. 143.28 Lat. 38.33
10	Geiyo	2001/03/24	6.7	51 km	Intraplate	Long. 132.71 Lat. 34.12
11	Iwateken nairikunanbu	2001/12/02	6.5	122 km	Intraplate	Long. 141.26 Lat. 39.40
12	Miyagiken oki	2003/05/26	7.0	70 km	Intraplate	Long. 141.68 Lat. 38.81
13	Surugawan	2009/08/11	6.2	23 km	Intraplate	Long. 138.50 Lat. 34.78

#### 4. RESULTS

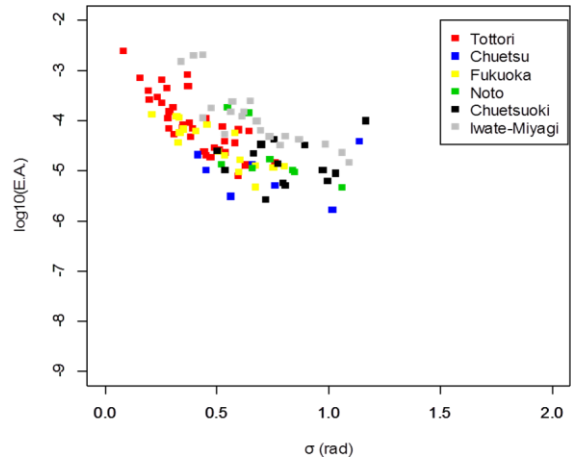
The  $\sigma$  and  $E.A.$  relations for crustal, interface and intraplate earthquakes are presented in Fig.3, Fig.4 and Fig.5, respectively. Following tendencies are observed:

- For all earthquake types, the slopes of the  $\sigma$  and  $E.A.$  relations are steeper for higher frequency band.
- The slopes are different for the different earthquake types (e.g. the slope in the interface earthquakes are less steep than the other two types in all frequency bands.)
- In frequency bands of 3.0 – 5.0 Hz and higher, all earthquakes in the same type show similar  $\sigma$  and  $E.A.$  relations regardless of the earthquake magnitude and depth. In other three frequency bands, shallower or larger-magnitude earthquakes show higher  $\sigma$  for the same  $E.A.$  The tendencies were also reported in Ishii and Watanabe (1987). However, to ensure the validities of those tendencies, more earthquakes should be analyzed.
- As expected, the  $\sigma$  and  $E.A.$  relations are very different between the sedimentary sites and non-sedimentary sites in 0.1 – 1.0 Hz. In general, in sedimentary sites, the  $\sigma$  and  $E.A.$  relations are flatter.

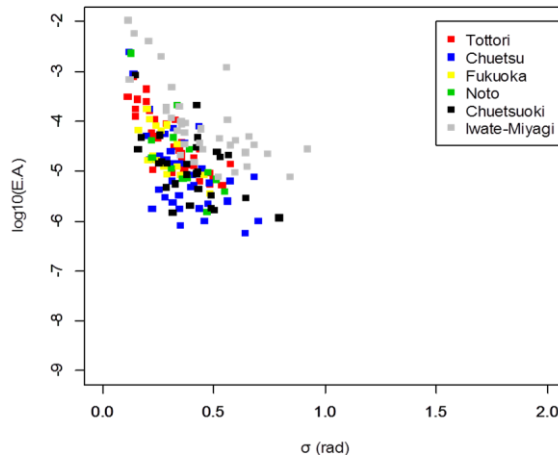
As for the  $D$  and  $E.A.$  relations, the authors defined six groups in chapter 2. Some examples of the  $D$  and  $E.A.$  relations are shown in Fig.6. Note that different groups show clearly different  $E.A.$  for the same  $D$ . Generally speaking, sites in Group 6 show the highest  $E.A.$  values, while sites in Group 1 show the lowest for the same  $D$  values.



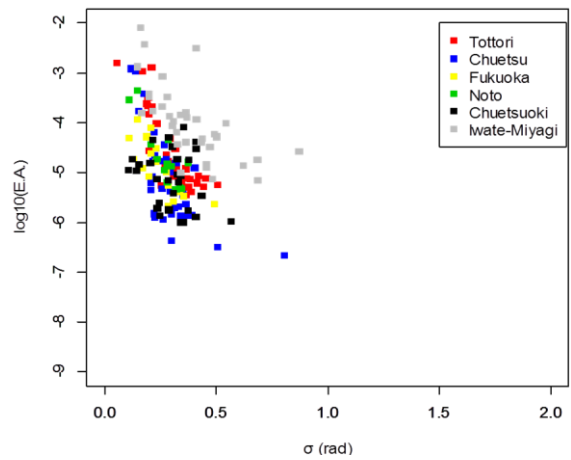
a) 0.1 – 1.0 Hz (sedimentary)



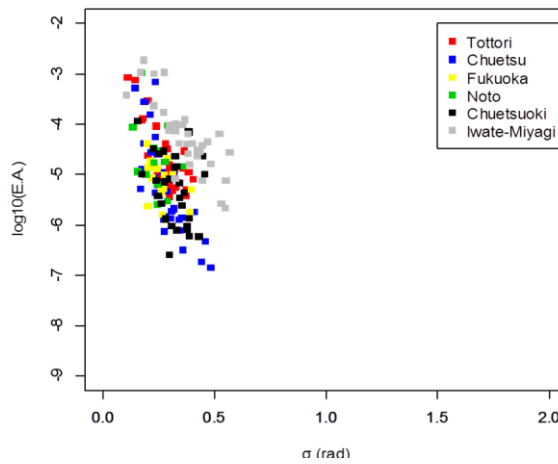
b) 0.1 – 1.0 Hz (non-sedimentary)



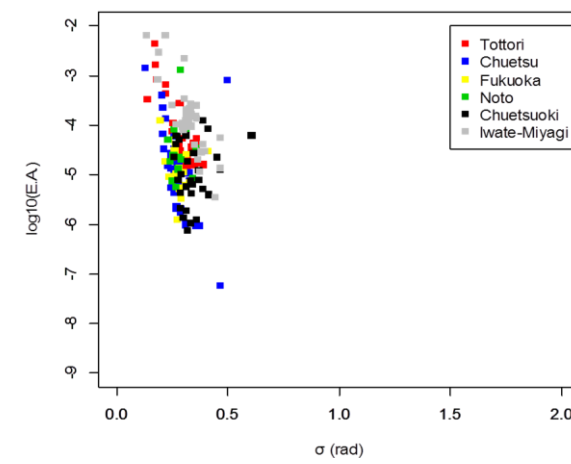
c) 1.0 – 2.0 Hz



d) 2.0 – 3.0 Hz

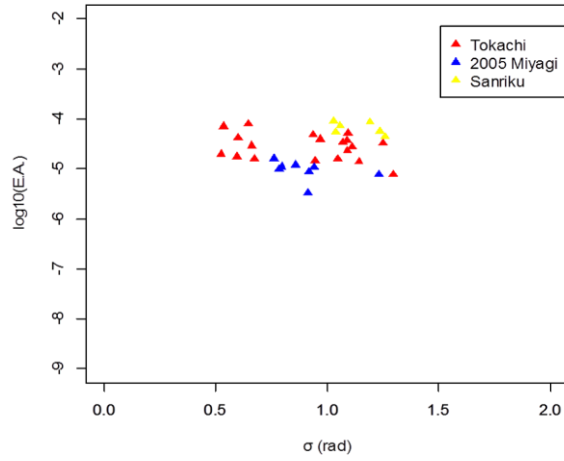


e) 3.0 – 5.0 Hz

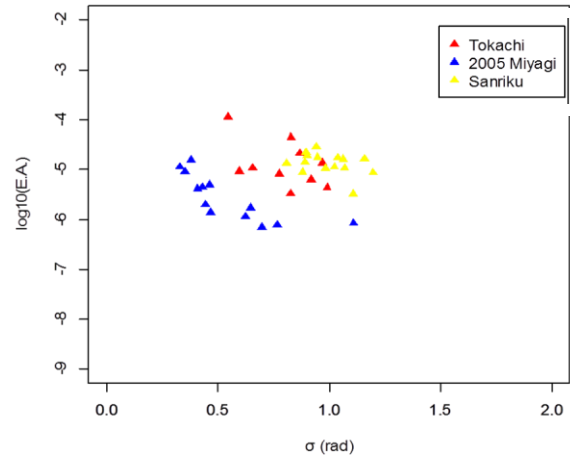


f) 5.0 – 10.0 Hz

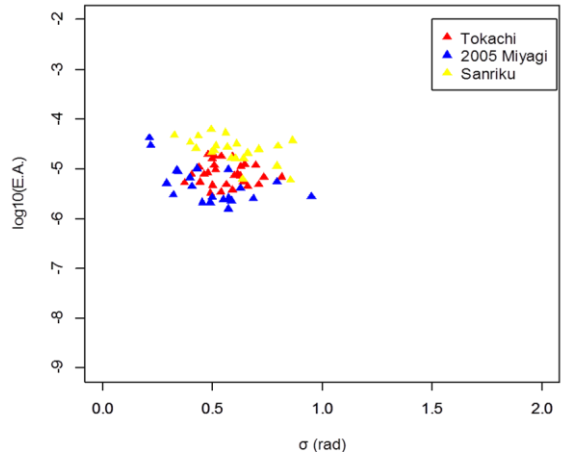
**Figure 3.** Relation of  $\sigma$  and  $E.A.$  in crustal earthquakes in each frequency



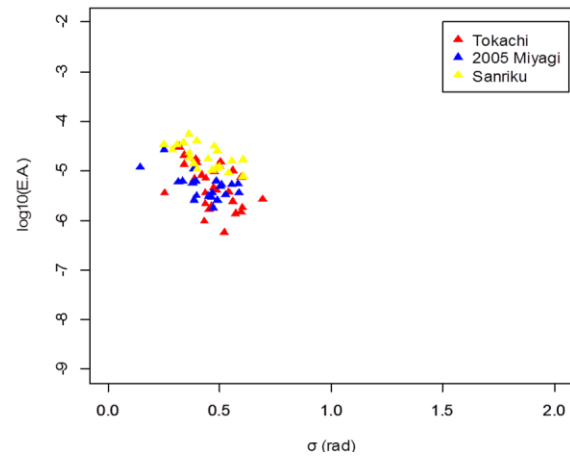
a) 0.1 – 1.0 Hz (sedimentary)



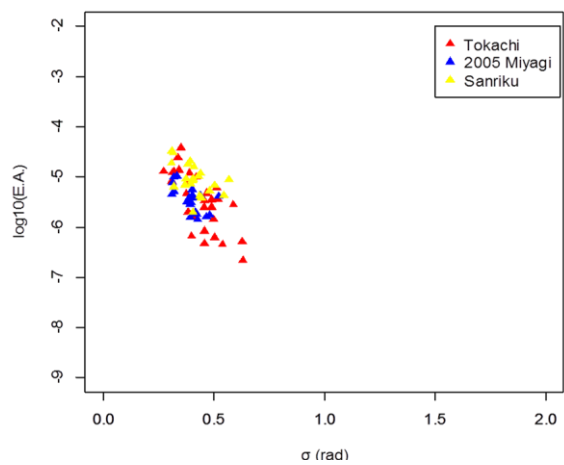
b) 0.1 – 1.0 Hz (non-sedimentary)



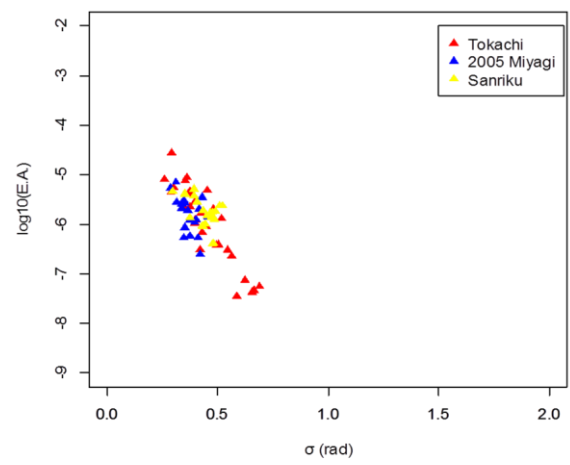
c) 1.0 – 2.0 Hz



d) 2.0 – 3.0 Hz

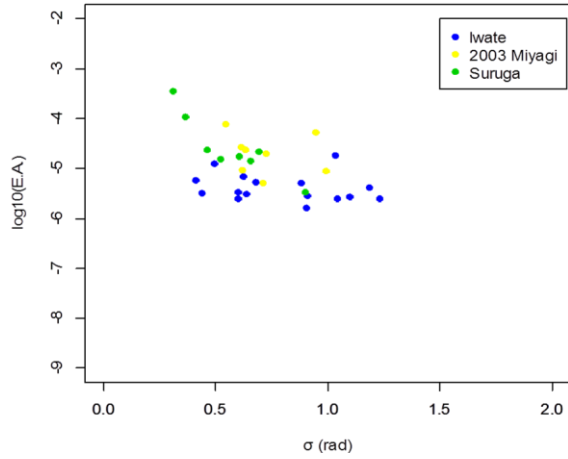


e) 3.0 – 5.0 Hz

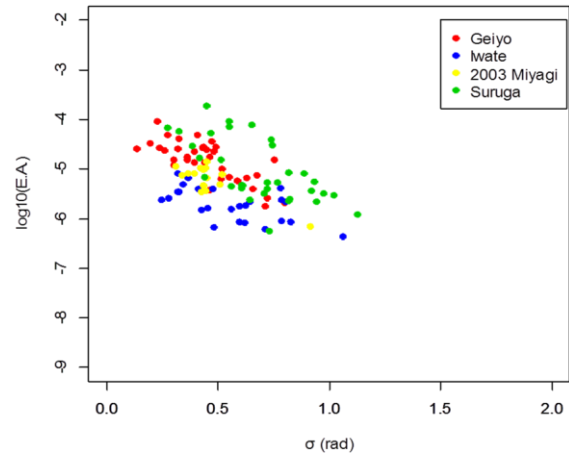


f) 5.0 – 10.0 Hz

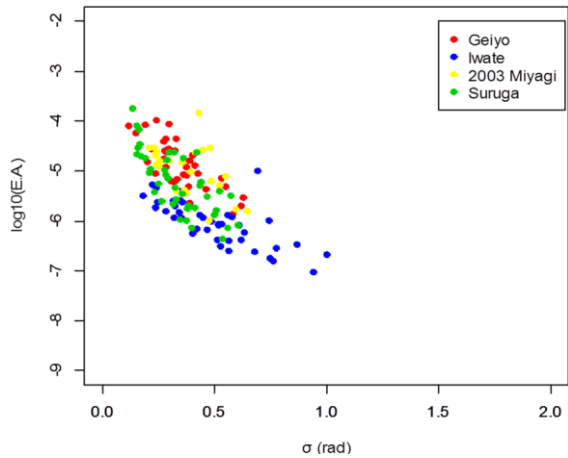
**Figure 4.** Relation of  $\sigma$  and  $E.A.$  in interface earthquakes in each frequency



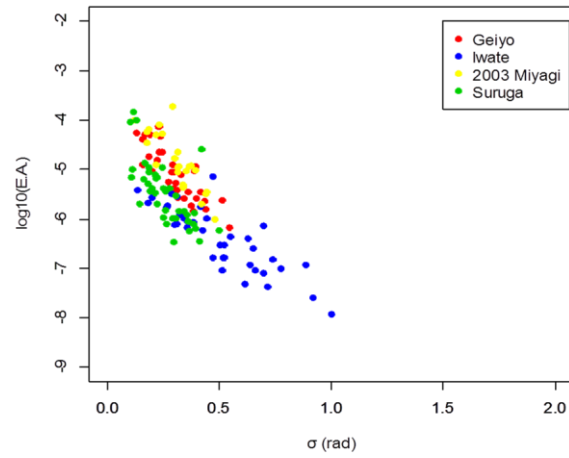
a) 0.1 – 1.0 Hz (sedimentary)



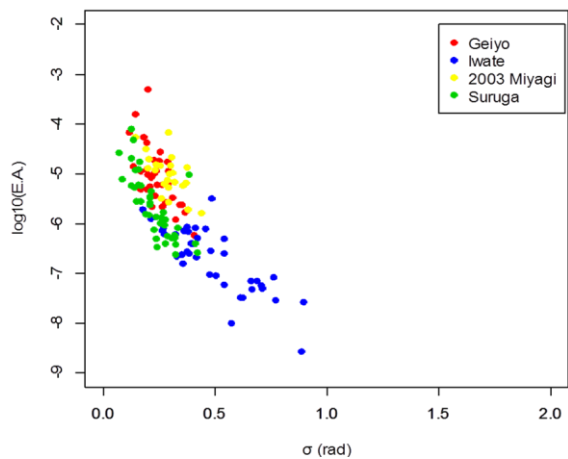
b) 0.1 – 1.0 Hz (non-sedimentary)



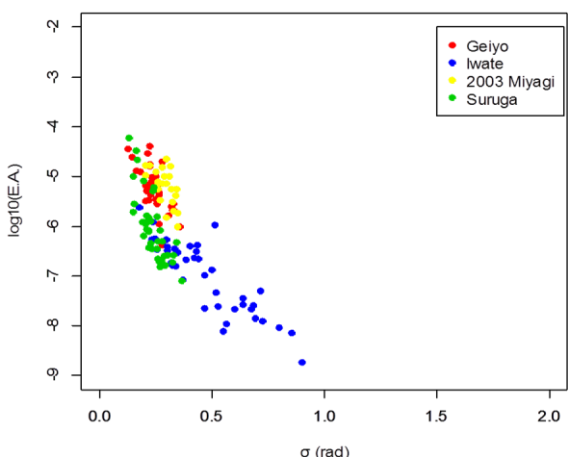
c) 1.0 – 2.0 Hz



d) 2.0 – 3.0 Hz

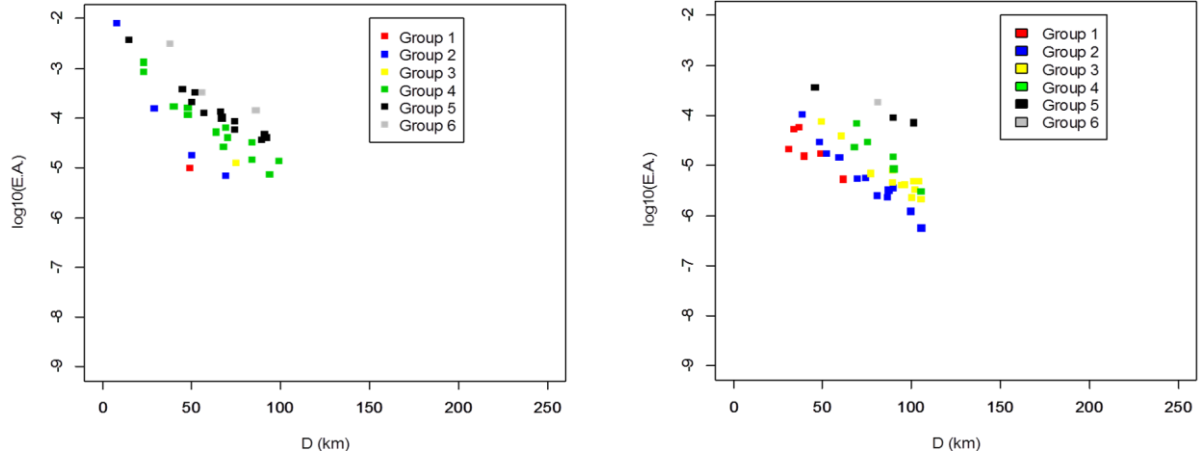


e) 3.0 – 5.0 Hz



f) 5.0 – 10.0 Hz

**Figure 5.** Relation of  $\sigma$  and  $E.A.$  in intraplate earthquakes in each frequency band



a) 2008 Iwate-Miyagi earthquake, 2.0 – 3.0 Hz      b) 2009 Surugawan earthquake, 0.1 – 1.0 Hz

**Figure 6.** Examples of the  $D$  and  $E.A.$  relations

## 5. NUMERICAL EXAMPLES

The authors developed a ground motion simulation flowchart. The flowchart is shown in Fig.7. In Step 1, one needs to assume the hypocentral location, depth, rupture mechanism (crustal, interface or intraplate) and moment magnitude as well as the construction site. In Step 2, referring to researches on the Q-factor, which “Group” the construction site belongs to can be determined in each frequency band. From this information,  $E.A.$  and thus the spectral intensity level can be computed in each frequency band (Step 3). In Step 4, the design Fourier spectrum having the expected spectral intensities can be assumed.

As for the phase, the standard deviation ( $\sigma$ ) of the phase difference can be estimated from the  $E.A.$  (Step 5). Note that in low frequency band such as 0.1 – 1.0 Hz, the  $\sigma$  and  $E.A.$  relation is different for sedimentary and non-sedimentary sites. For the higher moments (skewness ( $\beta_3$ ) and kurtosis ( $\beta_4$ )), the authors show that  $\sigma$  and  $\beta_3$ , and  $\sigma$  and  $\beta_4$  are correlated (Nagao and Kanda (2012)). Therefore, in Step 6,  $\beta_3$  and  $\beta_4$  are estimated from  $\sigma$ . By setting appropriate  $\mu$  (mean) value, one can model phase differences in each frequency band (Step 7). In Step 8, the ground motion is complete by taking the inverse Fourier transform of the simulated phase and Fourier spectrum. Using the flowchart, the authors simulated three artificial ground motion cases. The assumed parameters are in Table.2 and simulated ground motion cases are in Fig.8. Note that in case 2, the ground motion has a long duration and its long-period-contents are strong.

**Table 2.** Parameters of examples in this study

#	Type	$M_w$	Depth (km)	Hypocenter	D (km)	Group	Sedimentary layer?
1	crustal	6.6	10	Long. 133.35 Lat. 35.28	30	3 in all bands	No
2	interface	7.9	45	Long. 144.07 Lat. 41.78	150	5 in all bands	Yes
3	intraplate	6.2	25	Long. 138.50 Lat. 34.78	50	2 in all bands	No

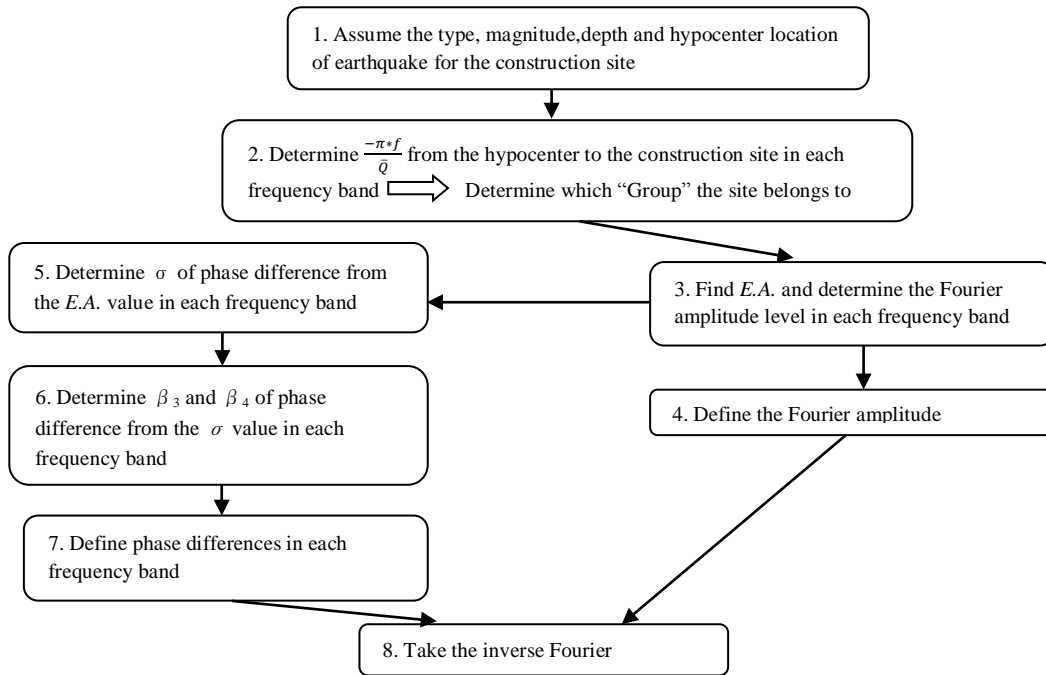


**Figure 7.** Flowchart to generate the design ground motion based on this research

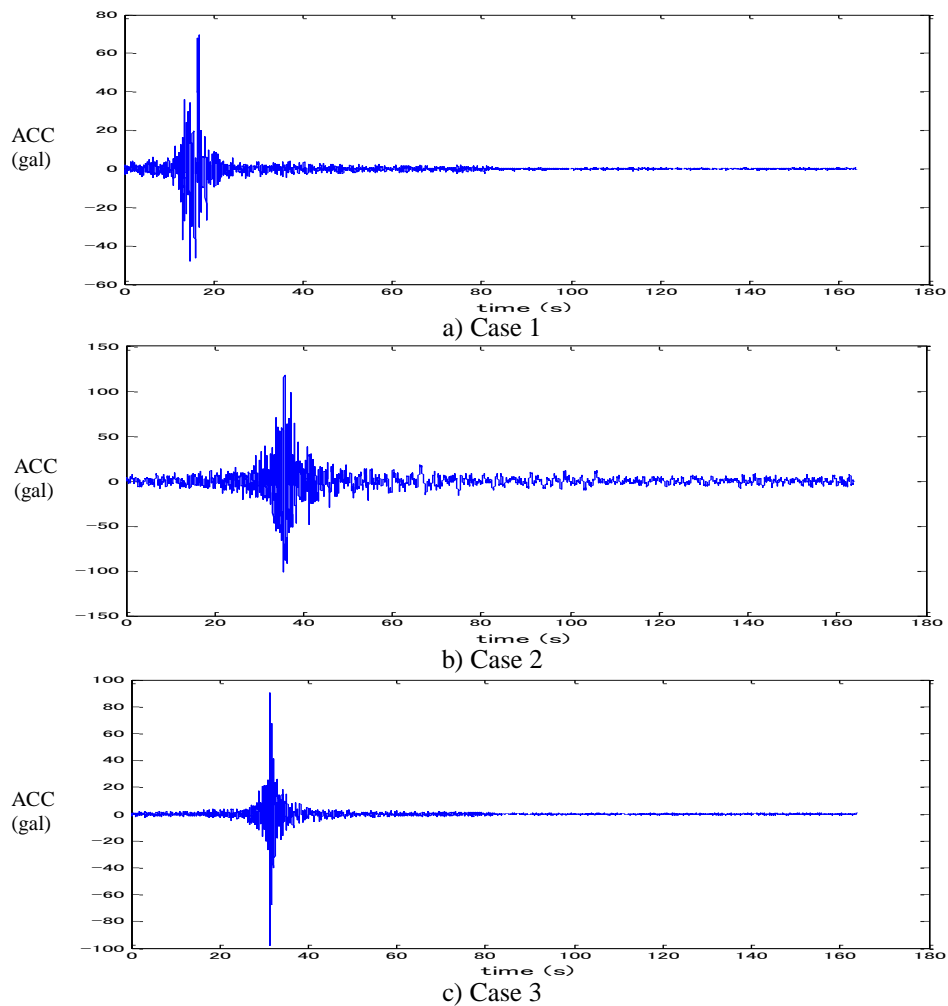


**Figure 8.** Simulated ground motion cases

## 6. CONCLUSIONS

In this paper, the authors defined the *E.A.*, which can take into account the heterogeneous *Q* and *V<sub>s</sub>* values, to estimate the standard deviation of the phase difference. Although the relations are to some extent different for the different earthquake types (in all frequency bands), the different depths and magnitudes (up to 2 – 3 Hz) and the different frequency bands, the standard deviation and *E.A.* have clear relations, which enables one to estimate the standard deviation from the *E.A.* In the final part of this paper, the three numerical examples are demonstrated. In the flowchart, the characteristics of the four moments of phase differences are utilized to model the phase angles for the simulated ground motions.

## REFERENCES

- Boore, D.M. (1983). Stochastic simulation of high-frequency ground motions based on seismological models of the radiated spectra. *Bull. Seism. Soc. Am.* **73**, 1865 – 1894.
- Ishii, T. and Watanabe, T. (1987). Relations between phase characteristics of ground motions and magnitudes, focal distances and focal depths of earthquakes. *Proc. Annual Meeting, Archit. Inst. Japan* **B1**, 385 – 386 (in Japanese).
- Iwasaki, R., Kanda, J., Masao, T. and Ohkawa, I. (1988). Fundamental properties of phase difference distribution for earthquake ground motions. *Archit. Inst. Japan* **386**, 16-23 (in Japanese).
- Nagao, K. and Kanda, J. (2012). Study on higher-moments' characteristics of phase difference of ground motion. *Proc. Annual Meeting, Archit. Inst. Japan*, in review (in Japanese).
- Nishikawa, T., Arakawa, T., Hisada, Y., Soda, S., Tohdoh, M., Yamamura, K. (2008). Vibration of architecture. Asakura Publishing Co., Ltd. (in Japanese).
- Ohsaki, Y. (1979). Study On the significance of phase content in earthquake ground motions. *Earthquake Eng. & Struct. Dynamics* **7:5**, 427 – 439
- Papoulis, A. (1977) Signal Analysis. McGraw-Hill, Inc.
- Sato, T. (2007). Attenuation of peak ground acceleration and peak ground velocity of statistical green's function. *J. Japan Association of earthquake engineering* **7:6**, 1 – 16 (in Japanese).
- Yamane, T. and Nagahashi, S. (2002). A study on a generation of simulated earthquake ground motion considering phase difference characteristics: Part 1 Theoretical background of the relationship between phase difference distribution and envelope. *J. Archit. Inst. Japan* **553**, 49 – 56.